Geomechanics and Engineering, *Vol. 12, No. 5 (2017) 831-847*
DOI: https://doi.org/10.12989/gae.2017.12.5.831

Geotechnical shear behavior of Xanthan Gum biopolymer treated sand from direct shear testing

Sojeong Lee [1a], Ilhan Chang [*2], Moon-Kyung Chung [1b], Yunyoung Kim [3c] and Jong Kee [4d]

[1] *Geotechnical Engineering Research Institute (GERI), Korea Institute of Civil Engineering and Building Technology (KICT), 283 Goyangdae-ro, Goyang 10223, Republic of Korea*
[2] *School of Engineering and Information Technology, University of New South Wales (UNSW), Canberra, ACT 2600, Australia*
[3] *Inha University, 100 Inha-ro, Incheon 22212, Republic of Korea*
[4] *Hanyang University, 55 Hanyangdaehak-ro, Ansan 15588, Republic of Korea*

(*Received October 14, 2016, Revised January 06, 2017, Accepted February 14, 2017*)

Abstract. Conventional geotechnical engineering soil binders such as ordinary cement or lime have environmental issues in terms of sustainable development. Thus, environmentally friendly materials have attracted considerable interest in modern geotechnical engineering. Microbial biopolymers are being actively developed in order to improve geotechnical engineering properties such as aggregate stability, strength, and hydraulic conductivity of various soil types. This study evaluates the geotechnical engineering shear behavior of sand treated with xanthan gum biopolymer through laboratory direct shear testing. Xanthan gum-sand mixtures with various xanthan gum content (percent to the mass of sand) and gel phases (initial, dried, and re-submerged) were considered. Xanthan gum content of 1.0% sufficiently improves the inter-particle cohesion of cohesionless sands 3.8 times and more (up to 14 times for dried state) than in the untreated (natural) condition, regardless of the xanthan gum gel condition. In general, the strength of xanthan gum-treated sand shows dependency with the rheology and phase of xanthan gum gels in inter-granular pores, which decreases in order as dried (biofilm state), initial (uniform hydrogel), and re-submerged (swollen hydrogel after drying) states. As xanthan gum hydrogels are pseudo-plastic, both inter-particle friction angle and cohesion of xanthan gum-treated sand decrease with water adsorbed swelling at large strain levels. However, for 2% xanthan gum-treated sands, the re-submerged state shows a higher strength than the initial state due to the gradual and non-uniform swelling behavior of highly concentrated biofilms.

Keywords: Xanthan gum; biopolymer; direct shear; inter-particle; friction angle; cohesion

1. Introduction

In geotechnical engineering, soil treatment for strength improvement is an essential prerequisite for most construction and building practices. Deep mixing, using cement or lime, is a commonly applied method in various ground improvement implementations to enhance foundation stabiliza-

*Corresponding author, Lecturer, E-mail: ilhan.chang@adfa.edu.au
[a] Research Specialist, E-mail: sojunglee513@kict.re.kr
[b] Senior Research Fellow, E-mail: mkchung@kict.re.kr
[c] Student, E-mail: kyy2233@naver.com
[d] Student, E-mail: keejong0523@hanyang.ac.kr

 ISSN: 2005-307X (Print), 2092-6219 (Online)

tion (Shooshpasha and Shirvani 2015) and to prevent in-situ soil erosions (Broms and Boman 1975). Deep mixing can be classified into DCM (Deep Cement Mixing) and DLM (Deep Lime Mixing) methods according to the main binder material used. Since the DCM method was developed in the 1960s, DCM has been widely applied in various inland and offshore constructions due to its advanced field machinery equipment and cumulated experiences on in-situ operation and quality control (Horpibulsk *et al*. 2011, Lin and Wong 1999). As a result, DCM constructions have rapidly increased, with 2004 showing some 55 million m^3 of accumulated soil treatment around the world, and approximately 17.6 million m^3 in Korea alone (Druss 2005).

DLM is more common than DCM in Europe. In Finland and Sweden, DLM is actively performed by improving more than 300,000 m^3 of ground every year (Bergado 1996). In the U.S.A., DLM is mainly applied in highway construction sites by treating more than 500,000 m^3 of soil per annum (Ahn 2010, Jeong *et al*. 2009). When lime is mixed with soil via DLM construction, the calcium hydroxide ($Ca(OH)_2$) in lime causes slaking and flocculation (Boardman *et al*. 2001, Larsson *et al*. 2009). However, the formation of ettringite ($Ca_6Al_2(SO_4)_3(OH)_{12}26H_2O$) via lime hydration increases the soil pH, which disrupts vegetation growth in soil and accelerates land degradation (Havlica and Sahu 1992, Malekpoor and Poorebrahim 2014).

Among several environmental concerns of DCM and DLM ground improvement methods, greenhouse gas emission related to the use of conventional binders (especially ordinary cement) has become a serious threat to the global environment (Chang *et al*. 2016b). In particular, CO_2 emission related to cement production and utilization is reported to occupy 7~8% of the entire global CO_2 emissions (Chang *et al*. 2016b, 2015b). The U.S. Energy Information Administration notes that 61 million tons of CO_2 emission can be reduced if 10% of cement usage in the construction field is replaced with alternative materials (Choate 2003, U.S. Energy Information Administration 2015).

Thus, the development of environmentally friendly, geotechnical construction material is necessary with respect to sustainable geotechnical engineering (Chang *et al*. 2016b, 2015d). Recently, microbial biopolymers (high molecular polysaccharides produced by microbes) have been introduced and trialed as new geotechnical engineering binders to reduce the usage of conventional binders (Ayeldeen *et al*. 2016, Chang *et al*. 2016b). Biopolymer treatment shows a higher strengthening efficiency and performance than concurrent microbial precipitation methods such as MICP (microbial induced calcite precipitation) (Cole *et al*. 2012). Biopolymers show remarkable strengthening due to the direct ionic bonding between biopolymers and fine particles (Chang and Cho 2012, 2014, Chang *et al*. 2015a) or continuous biopolymer matrix formation between coarse particles (Chang *et al*. 2016a, C2015c, Ham *et al*. 2016). Moreover, biopolymer application is expected to decrease the CO_2 emission related to the construction industry due to the reduction of cement usage and carbon fixation via biopolymer production (Chang and Cho 2012, Chang *et al*. 2016b).

Gel-type xanthan gum biopolymer is one example of a biopolymer that shows strong potential for practical implementation due to its sufficient strengthening (Ayeldeen *et al*. 2016, Chang *et al*. 2015a, Nugent *et al*. 2009) and good economic feasibility based on mass commercialization (Casas *et al*. 2000, Chang *et al*. 2015b). In this study, the geotechnical engineering shear behavior of xanthan gum-treated sand is evaluated via laboratory direct shear testing. Xanthan gum-sand mixtures with varied xanthan gum content (percent to the mass of sand) and gel phases (initial, dried, and re-submerged) were considered in order to investigate the inter-particle interaction between xanthan gum biopolymer and cohesionless sand based on peak and residual behavior analyses.

2. Materials and methods

2.1 Materials

2.1.1 Sand: *Jumunjin standard sand*

Jumunjin sand is used as the target cohesionless sand in this study. Jumunjin sand is a standard sand in Korea, classified as *SP* due to its particle size distribution, as shown in Fig. 1. The detailed representative basic soil properties of jumunjin sand are summarized in Table 1.

2.1.2 Xanthan Gum biopolymer

Xanthan gum is a polysaccharide created by *Xanthomonas campestris* bacteria, and is a commonly used biopolymer in various industrial fields. Xanthan gum is a hetero-polysaccharide; its structure consists of two glucoses, two mannoses, and one glucuronic acid (penta-saccharide). Xanthan gum is an anionic biopolymer which easily adsorbs water molecules via hydrogen bonding, and which mainly forms viscous hydrogels (García *et al*. 2011). Thus, xanthan gum is commonly used as fluid thickeners in the food industry and as an additive for drilling muds in the mining and petroleum industries due to its significant viscosity increase in only a small amount (Chang *et al*. 2015a). Moreover, xanthan gum has been suggested to be used in excavation slurries for machinery tunneling such as slurry-shield TBM (Tunnel Boring Machnie) practices (Comba and Sethi 2009).

2.1.3 Gypsum

Gypsum can be classified as gypsum dihydrate ($CaSO_4 \cdot 2H_2O$), gypsum hemihydrate ($CaSO_4 \cdot 1/2H_2O$), and anhydrous gypsum ($CaSO_4$). Ordinarily, the word gypsum refers to gypsum hemihydrate. Gypsum hemihydrate is obtained by baking dihydrate, and anhydrous gypsum is derived as a byproduct by baking gypsum hemihydrate. The gypsum used in this study is gypsum

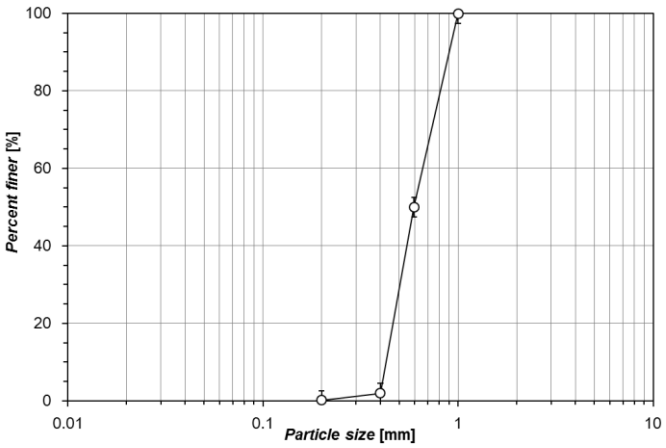

Fig. 1 Particle size distribution of jumunjin sand

Table 1 Basic geotechnical engineering properties of Jumunjin sand

C_u	C_c	e_{max}	e_{min}	G_s	*USCS*
1.94	1.09	0.89	0.64	2.65	SP

hemihydrate, and its pure hydrated specimen shows approximately 7.4 MPa unconfined compressive strength in the case of moist curing, while its strength increases up to 13.7 MPa in the case of dry curing. The volumetric expansion strain via gypsum hydration is around 0.12%, which becomes negligible when mixed with sandy soils.

2.2 Experimental methods

2.2.1 Specimens preparation

Pure (untreated) sand, xanthan gum-treated sand, and gypsum-treated sand specimens are used for the experimental procedures in this study. Xanthan gum-treated sand specimens were prepared with 0.5%, 1.0%, and 2.0% xanthan gum contents to the mass of sand. For references, untreated pure sand and gypsum-treated sand specimens were prepared simultaneously.

Xanthan gum-treated sand specimens were prepared by mixing clean and dry sand with xanthan gum solutions (hydrocolloids). Purified xanthan gum (Sigma-Aldrich®, CAS No. 11138-66-2) was dissolved in distilled water at room temperature. According to the desired 20% initial water content, and 0.5%, 1.0%, and 2.0% xanthan gum contents to the mass of sand, 2.5%, 5.0%, and 10.0% xanthan gum solutions (xanthan gum content to the mass of water) were prepared respectively. A laboratory magnet stirrer was used to provide uniform xanthan gum solutions.

After uniform dissolution, xanthan gum solutions were thoroughly mixed with dry sand. Xanthan gum-sand mixture was poured and molded into a disk shape having dimensions of 60 mm in diameter and 20 mm in height, to be appropriated for direct shear testing. The initial relative density of the xanthan gum-treated specimens was controlled to be within a D_r range of 0.85~0.89 via tapping, to minimize the effect of different particle composition on strengthening. The molded xanthan gum-treated sand specimens were tested immediately without any drying to represent the "initial" state. Meanwhile, other xanthan gum-treated sand specimens were dried at room temperature for 28 days to represent the "dried" condition, while half of the dried specimens were submerged under distilled water at room temperature for 24 hours before performing direct shear testing to represent the "re-submerged" condition.

For the gypsum-treated sand specimens, gypsum-treated sand specimens were carried out for two cases with 10% and 20% gypsum-to-sand content, due to the typical range (5 to 10%) of gypsum applied in geotechnical engineering practices (Bell 1996, Plank 2005, Sherwood 1993). To match the same initial water content of the xanthan gum-treated sand specimens (20%), gypsum pastes were prepared by mixing gypsum powder with distilled water at 200% and 100% water-to-gypsum ratios (in mass). Then, the gypsum pastes were uniformly mixed with clean sand and molded into a disk shape having identical dimensions (60 mm in diameter and 20 mm in height) and initial relative density (D_r = 0.85) values in accordance with those of xanthan gum-treated specimens. Molded gypsum-treated sand specimens were cured at room temperature for 28 days before testing.

2.2.2 Direct shear testing

All disk shape (D 60 mm × H 20 mm) untreated, xanthan gum-treated, and gypsum-treated sand samples were placed into a direct shear apparatus (Humboldt HM-2560A) with porous stones placed above and beneath, and confined with 50, 100, 200, and 400 kPa vertical confinement respectively via a pneumatic actuator until the vertical strain converged to a stable state before applying horizontal shear. The shear box remained dry for initial and dried conditions, while it was filled with distilled water for the re-submerged condition of the xanthan gum-treated sands. For the

re-submerged condition, all xanthan gum-treated sand specimens were continuously saturated for 24 hours before shearing, which is regarded to induce full saturation (degree of saturation > 99%). Vertical deformation due to the vertical confinement occurred instantly and finished within 5 minutes following load application. Thus, even though xanthan gum treatment provides artificial cohesion to cohesionless sand, consolidation consideration becomes negligible due to the immediate deformation behavior of xanthan gum-treated sands.

For each vertical confinement, horizontal shear was applied with a constant shear rate of 1.2 mm/min for 750 seconds to reach 25% horizontal shear deformation at maximum (ASTM D3080 / D3080M-11 2011). These experiments are conducted for 7.5 minutes, until the horizontal deformation becomes 15 mm. Horizontal load, vertical strain, and horizontal displacements were obtained automatically via load cell (HM-2300.020) and LVDT (Linear Variable Differential Transformer) (HM-14368, HM-14180) measurements. At least three different measurements were performed and averaged to represent the peak shear strength (τ_{peak}) and residual shear strength (τ_{res}) values for each single condition.

3. Experimental results

3.1 Direct shear strength of Xanthan Gum-Treated Sand

Typical horizontal displacement (δ)-direct shear stress (τ) behaviors of untreated, xanthan gum-treated, and gypsum-treated sands at dried condition are presented in Fig. 2. The peak shear strength (τ_{peak}) of the 20% gypsum-treated sand is noticeably higher than the others, and the 1% and 2% xanthan gum-treated sands show a higher τ_{peak} than that of the 10% gypsum-treated sand, which is even similar to the τ_{peak} of the untreated sand (Fig. 2(a)). Moreover, the volumetric strain (ε_v)-horizontal displacement (δ) behavior of the untreated and 20% gypsum-treated sands shows high dilation, while the 10% gypsum and xanthan gum-treated sands show lower dilatancy (Fig. 2(b)). This seems to be affected by the rigidity and continuity of cementitious materials in inter-granular pore spaces. Although xanthan gum gels become thin and firm biofilms via dehydration, the elastic stiffness and strength of ductile xanthan gum biofilms become extremely lower than those of brittle hydrated gypsum.

Moreover, the experimental result implies that 10% gypsum treatment is insufficient to fully fill

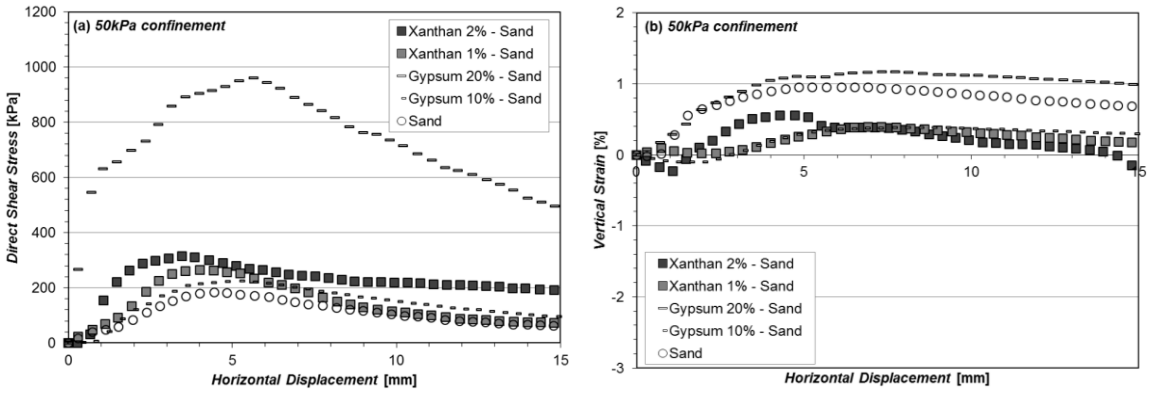

Fig. 2 Representative stress-strain relationship of xanthan / gypsum-treated sand

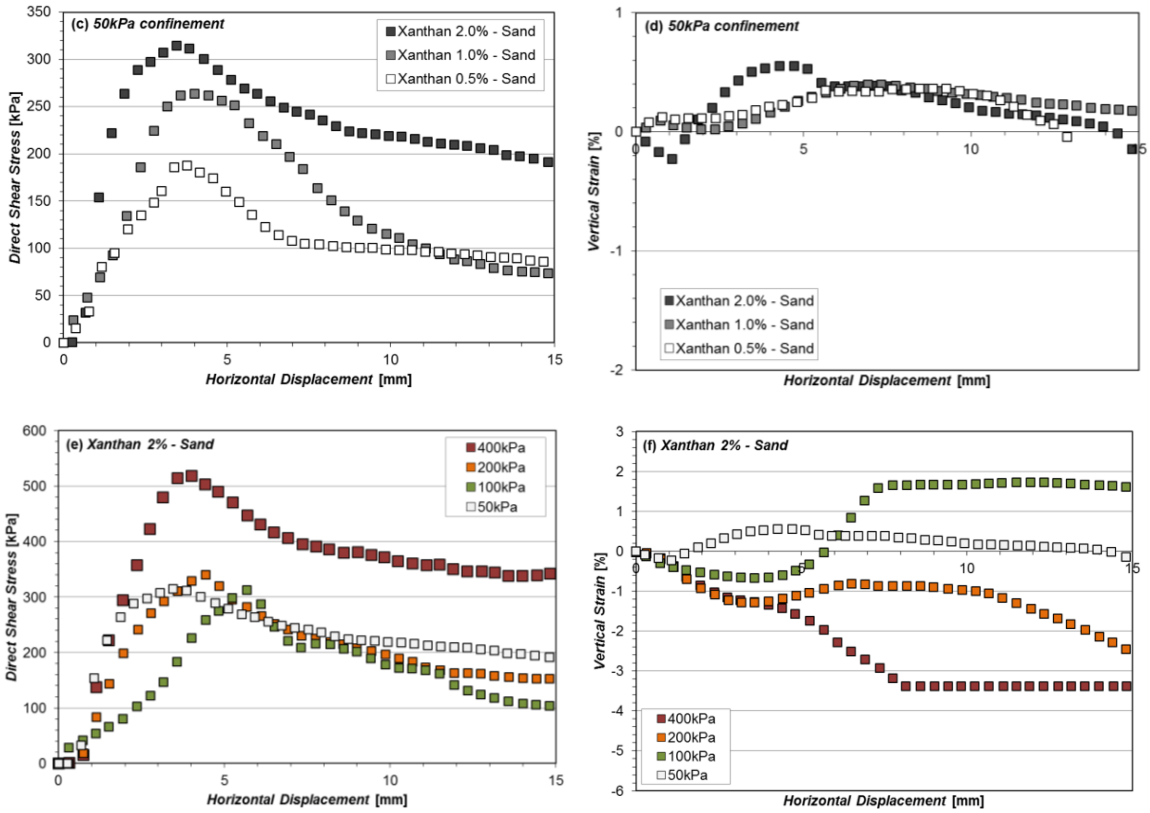

Fig. 2 Continued

inter-granular pores to build a continuous hydrated gypsum matrix which 20% gypsum treatment can form, and therefore shows low τ_{peak} value. Thus, it can be concluded that the typical range of lime mixing (around 10%) in practice is insufficient for improving the strength of cohesionless sandy soils.

Fig. 2(c) shows typical τ–δ curves of xanthan gum-treated sands with xanthan gum content increase. Although the 0.5% xanthan gum-treated sand becomes less effective on strengthening (τ_{peak} similar to untreated sand), τ_{peak} values gradually increase as xanthan gum content increases to 1% and 2%. Meanwhile, the ε_v–δ curves of the xanthan gum-treated sands (Fig. 2(d)) show a lower dilation than untreated sand, which seems to be affected by the ductility of the flexible biopolymer films existing between the sand particles.

Fig. 2(e) and (f) presents τ–δ and ε_v–δ relationships of the 2% xanthan gum-treated sand with vertical confinement variation. Indeed, τ_{peak} increases with higher confinement due to stronger interlocking between sand grains as well as sand grains and xanthan gum. Moreover, ε_v–δ curves show that xanthan gum-treated soil turns out to be contractive with vertical confinement increase.

3.2 Direct shear behavior of Xanthan Gum-Treated Sand with gel phase variation

Fig. 3 presents typical τ–δ and ε_v–δ relationships of xanthan gum-treated sands with different xanthan gum gel phases at initial (uniform hydrogel), dried (condensed biofilm), and re-submerged

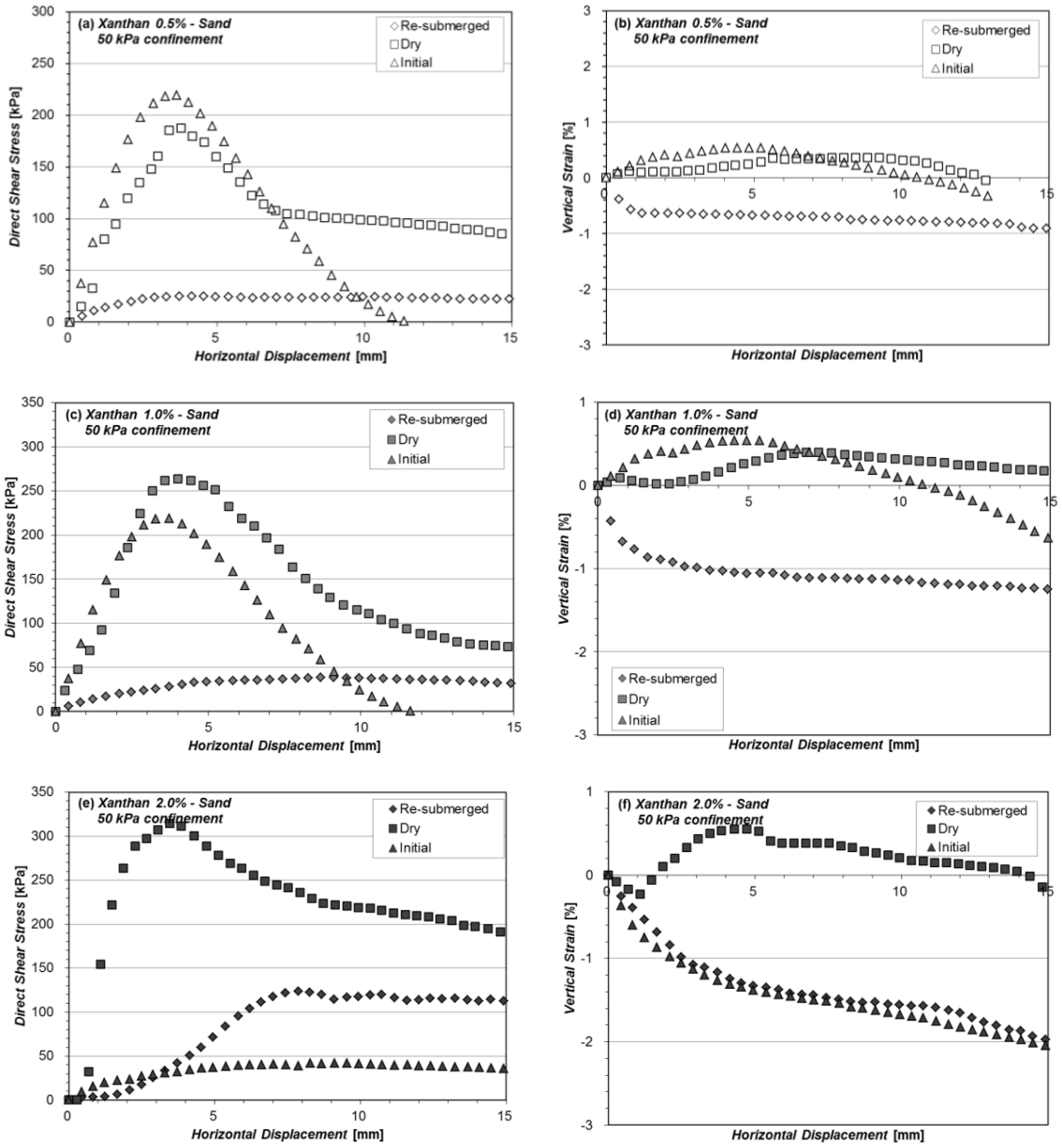

Fig. 3 Stress-strain relationship of xanthan-treated sand

(disturbed and swollen) conditions depending on the presence of water. Xanthan gum gels exist as a uniform hydrogel at the initial state (▲ symbols in Fig. 3) right after mixing with sand, which shows peak τ–δ behaviors for 0.5% and 1.0% xanthan gum content, but residual τ–δ behavior for 2.0% xanthan gum content.

With drying, xanthan gum hydrogels dehydrate and form thin and firm biofilms between sand grains with a larger portion of air in the voids (□ symbols in Fig. 3). The dried xanthan gum-treated sand shows peak τ–δ behavior, regardless of the xanthan gum content. The dried state

shows a higher τ_{peak} than the initial state except with 0.5% xanthan gum content. Moreover, both initial (220 kPa) and dried (190 kPa) τ_{peak} values of 0.5% xanthan gum-treated sand are close to the τ_{peak} of untreated sand (190 kPa). This implies that 0.5% xanthan gum content becomes insufficient to form continuous xanthan gum matrix inside soil, while xanthan gum contents higher than 1.0% show significant strengthening at dried state with the formation of continuous inter-granular xanthan gum matrix.

When the dried xanthan gum-treated sand is re-submerged into water (◊ symbols in Fig. 3), the condensed xanthan gum gels absorb water and swell due to their hydrophilicity resulting viscosity (or stiffness) reduction. For 0.5% and 1.0% xanthan gum contents, the τ_{peak} of the re-submerged conditions is remarkably lower than the initial and dried conditions (Figs. 3(a) and (c)), while 2.0% xanthan gum content shows a higher τ_{peak} for the re-submerged state rather than the initial state (Fig. 3(e)). The τ_{peak} differences between the initial and re-submerged conditions with different xanthan gum contents implies the different conditions of the xanthan gum hydrogels.

For all xanthan gum-treated sand mixtures, the initial water content was restricted at 20%, where initial gel concentration for the 0.5%, 1.0%, and 2.0% xanthan gum-treated sands were 2.5%, 5.0%, and 10.0%, respectively. Higher xanthan gum contents could render thicker xanthan gum biofilms in the dried condition. Thus, the high re-submerged τ_{peak} of the 2.0% xanthan gum-treated sand seems to be a result of the gradual and incomplete swelling of xanthan gum gels,

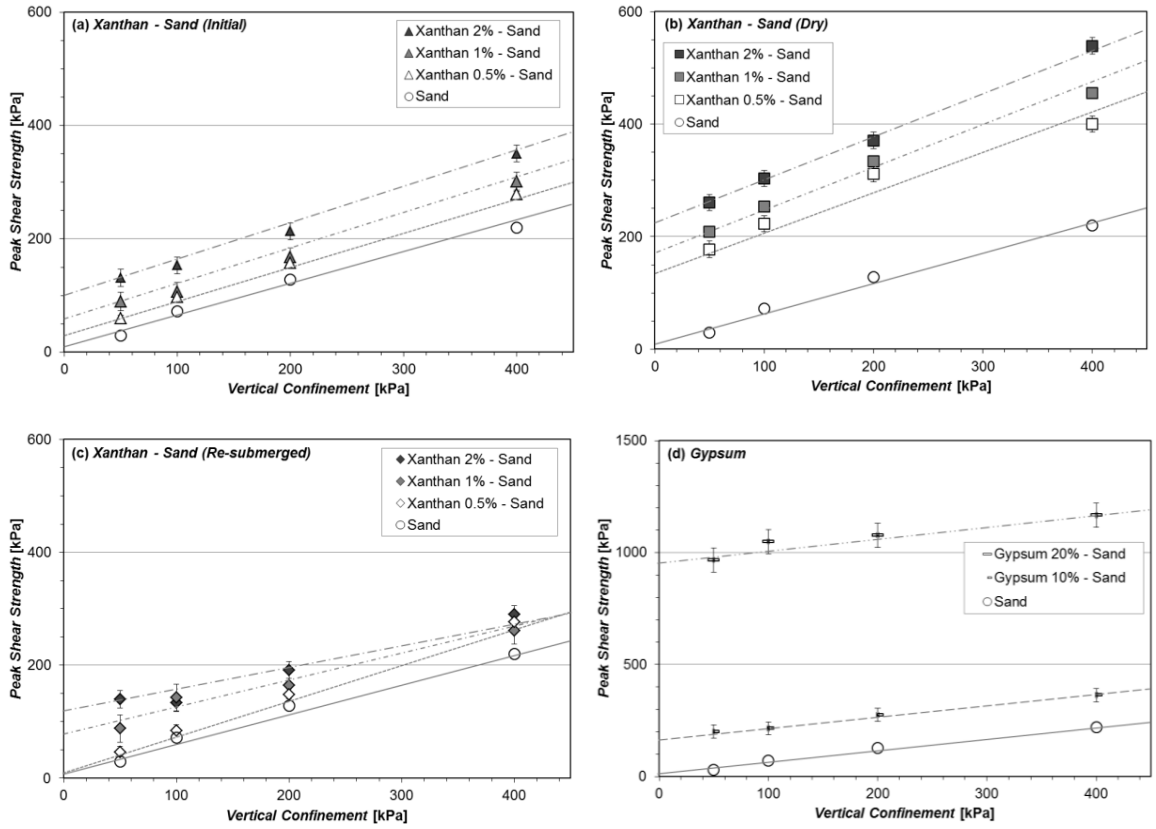

Fig. 4 Peak strength of xanthan gum-treated sand: (a) initial condition; (b) dry condition; (c) re-submerged condition; and (d) gypsum-treated sand

while 0.5% and 1.0% are expected to be completely swollen to weak hydrogels with lower concentrations compared to their initial concentration (2.5% and 5.0%) due to the presence of abundant water.

Fig. 4 presents the peak direct shear strength-vertical confinement (τ_{peak}-σ_v) curves to obtain the peak inter-particle cohesion (c_{peak}) and friction angle (ϕ_{peak}) values of xanthan gum-treated sands at initial, dried, and re-submerged conditions. τ_{peak} values increase with xanthan gum content increase, regardless of xanthan gum gel phase (water content), which is remarkable in initial and dry conditions, while the re-submerged condition becomes less sensitive with xanthan gum content variation.

Table 2 Peak behavior of xanthan gum-treated sand

Xanthan Gum content	Cohesion, c_{peak} [kPa]			Friction angle, ϕ_{peak}		
	Initial	Dry	Re-submerged	Initial	Dry	Re-submerged
0.0%	13.0	13.0	13.0	27.9	27.9	27.9
0.5%	34.3	160.6	15.5	31.5	32.1	32.0
1.0%	50.2	182.7	80.8	31.8	34.6	24.2
2.0%	92.6	218.4	107.2	32.5	38.4	22.4

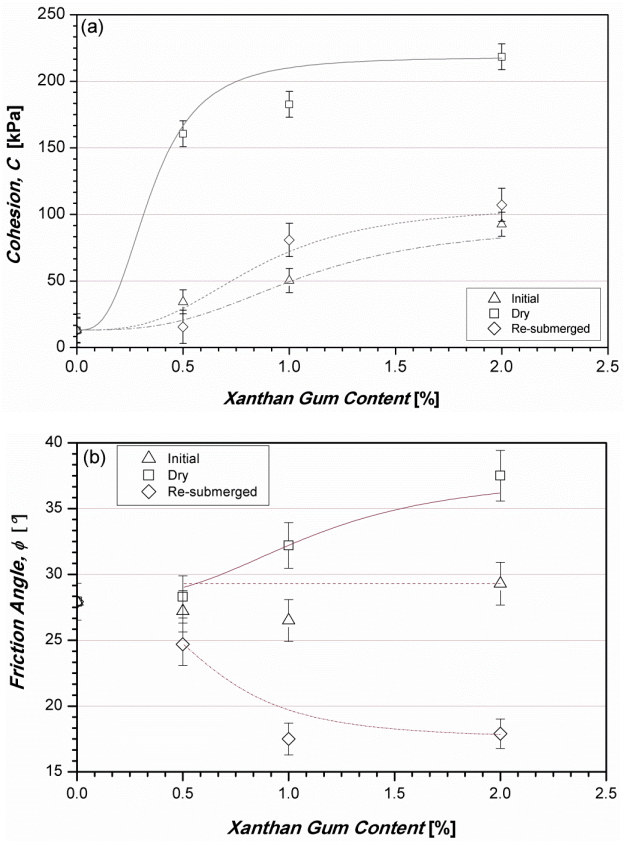

Fig. 5 Peak strength behavior of xanthan gum-treated sand: (a) cohesion; (b) friction angle

3.3 Peak shear strength properties of Xanthan Gum-Treated Sand

Both the c_{peak} and ϕ_{peak} values of xanthan gum-treated sands are summarized in Fig. 5 and Table 2. Only a small amount of xanthan gum (0.5%) renders different c_{peak} values, while ϕ_{peak} shows similar values at 0.5% xanthan gum content, regardless of the xanthan gum gel phases. At the initial condition, the presence of the xanthan gum gels increase c_{peak}, while ϕ_{peak} remains almost constant with xanthan gum content increase. This implies the strengthening mechanism of xanthan gum hydrogel to be mainly governed by the viscosity of xanthan gum gels for gel concentrations higher than 2.5%, without any effects on inter-particle friction behavior such as interlocking. For the dried condition, both the c_{peak} and ϕ_{peak} increase significantly due to the formation of firm xanthan gum biofilms via dehydration which are even higher than the 10% gypsum-treated sand (Fig. 5(d)).

Meanwhile, for the re-submerged condition, c_{peak} values are higher than those of the initial condition, for 1.0% and 2.0% xanthan gum contents. Thus, the aforementioned gradual and incomplete swelling behavior of xanthan gum gels (Section 3.2) seems to be also applicable for 1.0% xanthan gum content due to the higher c_{peak} for the re-submerged condition (Fig. 5(a)). However, ϕ_{peak} significantly decreases with xanthan gum increase for the re-submerged state (Fig. 5(b)), indicating a higher swelling pressure with higher xanthan gum contents which are attributed to significant inter-particle mechanical interaction (e.g., surface friction, interlocking) reductions.

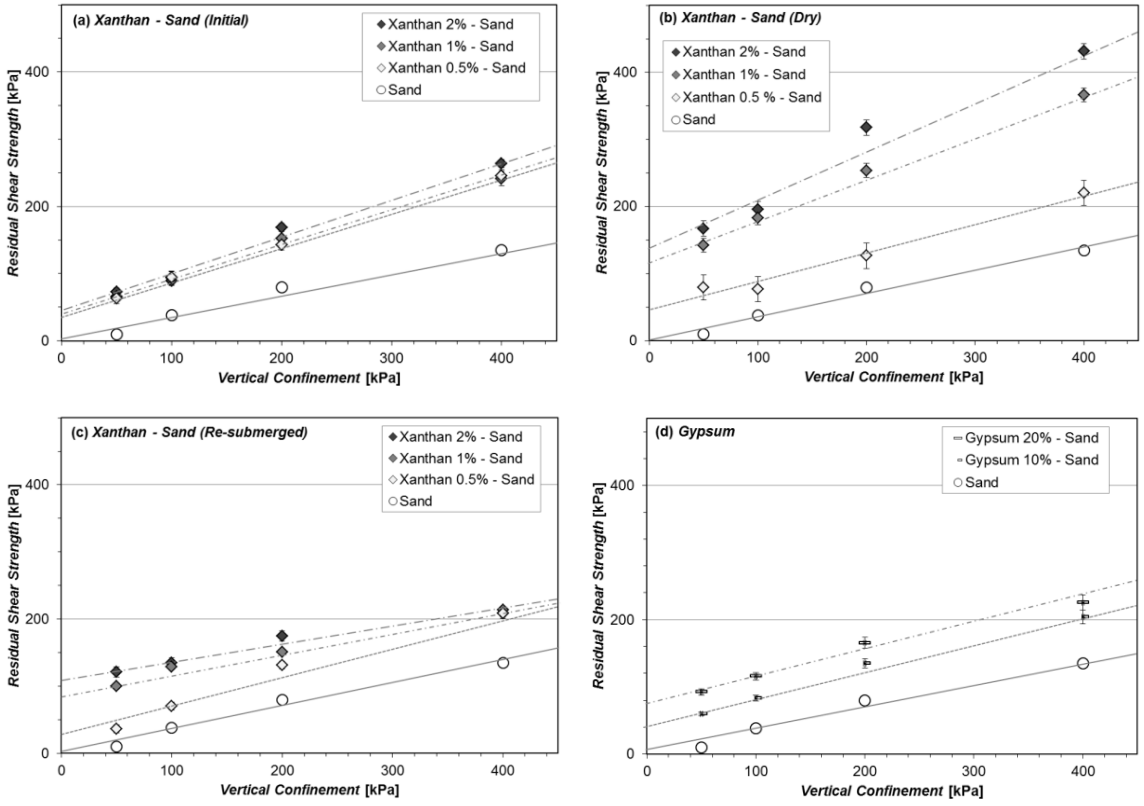

Fig. 6 Residual strength of xanthan gum-treated sand; (a) initial condition, (b) dry condition, (c) re-submerged condition, and (d) gypsum-treated sand

3.4 Residual shear strength properties of Xanthan Gum-Treated Sand

Fig. 6 presents the residual direct shear strength-vertical confinement (τ_{res}-σ_v) curves to obtain residual inter-particle cohesion (c_{res}) and friction angle (ϕ_{res}) values of xanthan gum-treated sands at initial, dried, and re-submerged conditions. Fig. 6 shows the τ_{res} increase of sands via xanthan gum treatment, regardless of the xanthan gum gel phases. For the dried condition, τ_{res} increases with higher xanthan gum contents (Fig. 6(b)), while xanthan gum-treated sands at the initial state show similar τ_{res} values, regardless of xanthan gum content (Fig. 6(a)).

Xanthan gum hydrogels at the initial state form a continuous xanthan gum matrix around sand grains via ionic bonding at rest. For large strain motions, xanthan gum hydrogels can be crushed into micro crumbs due to particle motions (e.g., shearing, rolling, and turning over). However, the constant c_{res} and ϕ_{res} values regardless of xanthan gum content (Fig. 7) implies the possibility of residual shear behavior to be affected by the van der Waals interaction (hydrogen bonding) between discrete xanthan gum hydrogels inside inter-granular pores along the shear band.

The increase of both c_{res} and ϕ_{res} of dried xanthan gum-treated sands seems to be attributed to the interaction between sand grains and xanthan gum fragments (crushed but still ductile). Moreover, the dried xanthan gum-treated sands show a higher τ_{res} than those of 10% and 20% gypsum-treated sands (Fig. 6(d)), which implies the remaining strengthening effect of ductile

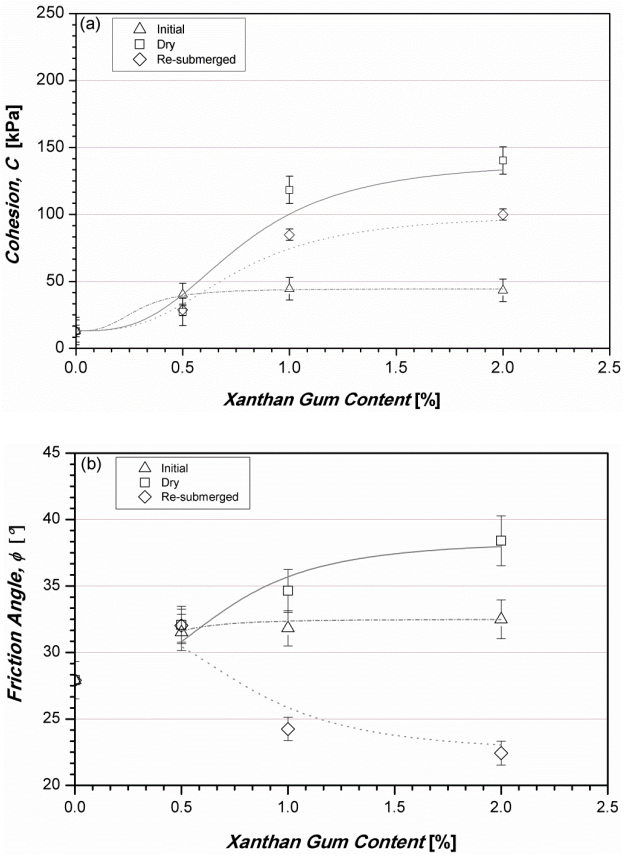

Fig. 7 Residual strength behavior of xanthan-treated sand: (a) cohesion; (b) friction angle

Table 3 Residual behavior of xanthan gum-treated sand

Xanthan Gum content	Cohesion, c_{res} [kPa]			Friction angle, ϕ_{res}		
	Initial	Dry	Re-submerged	Initial	Dry	Re-submerged
0.0%	13.0	13.0	13.0	27.9	27.9	27.9
0.5%	40.2	27.2	28.7	27.2	28.3	24.7
1.0%	44.5	118.3	84.8	26.5	32.2	17.5
2.0%	43.3	140.2	99.9	29.3	37.5	17.9

xanthan gum biofilms, while the strengthening effect of brittle gypsum hydrates diminishes at large shear strains.

The re-submerged xanthan gum-treated sand shows a c_{res} increase and ϕ_{res} decrease with higher xanthan gum contents (Fig, 7), which is similar to the peak behavior of the re-submerged xanthan gum-treated sands (Fig. 5). For the re-submerged condition, c_{peak} and c_{res} values show similar values (Tables 2 and 3), which shows the swelling behavior of dried xanthan gum gels to be non-uniform and independent to the level of strain (structural disturbance). Meanwhile, the notable ϕ_{res} reduction of the re-submerged xanthan gum-treated sands can be explained with the pseudo-plasticity of xanthan gum hydrogels acting as lubricants between sand grains due to the viscosity reduction at high strain levels.

4. Discussion

Generally, the shear behavior of cohesionless sand is mainly governed by inter-particle friction between sand grains (Das and Sobhan 2014, Mitchell and Soga 2005). Experimental results of this study show artificial cohesion on cohesionless sands provided by a xanthan gum biopolymer treatment. The friction angle variation of xanthan gum-treated soils show that xanthan gum treatment becomes mainly effective on inter-particle cohesion, rather than particle composition and structural alignment. Moreover, the artificial cohesion strongly depends on the phase of xanthan gum gels, where dried state (condensed biofilms) provides the strongest inter-particle strengthening. Meanwhile, xanthan gum-treated sand in the re-submerged condition has unique behaviors showing higher c_{peak} and c_{res} than those of the initial state, and considerable ϕ_{peak} and ϕ_{res} reduction with higher xanthan gum contents, while ϕ_{peak} and ϕ_{res} values of the initial state remain almost constant. Details are discussed in the following sections.

4.1 Geotechnical engineering behavior of Xanthan Gum-Treated Sand with gel phase (water content) variation

The different τ–δ behavior between 0.5%, 1.0% (peak behavior) and 2.0 (residual behavior) for xanthan gum-treated sands at the initial condition (Fig. 3) demonstrates the different inter-granular structural composition of xanthan gum-treated sands. The peak τ–δ behavior of the 0.5% and 1.0% xanthan gum-treated sands implies the inter-granular interaction between sand particles with 2.5% and 5.0% xanthan gum hydrogels in pore spaces to be still dominant on shear behavior. However, with 10.0% xanthan gum hydrogels in inter-granular pores, the high gel strength (viscosity) of highly concentrated hydrogels seems to mainly resist against shearing. In detail, for high xanthan gum hydrogel concentrations, the absolute strength (chemical bonding) of xanthan gum hydrogels

govern the shear resistance, which results in shear behavior similar to cohesive clayey soils. This indicates that the shear strength of xanthan gum-treated sand in the initial condition is mostly affected by the absolute hydrogel strength (concentration), due to the lack of direct interaction between xanthan gum hydrogels and electrically neutral sand grains (Chang *et al*. 2015a).

Meanwhile, when xanthan gum-treated sand is re-submerged in water, dried xanthan gum films absorb water and swell back to hydrogels, rendering residual τ–δ behaviors regardless of xanthan gum content (Fig. 3). However, τ_{peak} values of re-submerged conditions become lower τ_{peak} values at the initial state, except with 2.0% xanthan gum content. This refers to the distinctive swelling behavior of dried xanthan gum through re-hydration, where xanthan gum elements gradually swell and detach from the outside rim of the main biofilm body. For low xanthan gum contents, although gradual swelling can fully disturb and disperse xanthan gum into hydrogels, higher xanthan gum contents are expected to show remaining biofilm layers near sand particles with dispersed hydrogel layers above. This can explain the higher c_{peak} and c_{res} of the re-submerged xanthan gum-treated sand at the initial state for 1.0% and 2.0% xanthan gum contents, respectively.

4.2 Conceptual model for shearing behavior of Xanthan Gum-Treated Sand

The xanthan gum-treated sand behavior according to the gel phase is represented in Fig. 8. The experiments carried out are classified into three gel phase types—initial, dry, and re-submerged conditions.

In general, the peak shear strength is notable, as the amount of inter-particle contact increases in representative sand. Not only does the inter-particle adhesion between sand grains and xanthan gum hydrogels affect the overall shear strength of xanthan gum-treated sands, but also does the rheology (viscosity, shear strength) of xanthan gum hydrogels. With higher xanthan gum content, although the inherent strength of xanthan gum hydrogels increases, the particle composition of sand grains become loose due to the swelling of the xanthan gum hydrogels. However, the hydrogen bonding between sand grains and xanthan gum hydrogels is significantly low where xanthan gum hydrogels can easily detach (poor suspensibility) from the sand particle at both initial and re-submerged conditions. Meanwhile, water content at the initial state is defined, while the re-submerged state has no limitations except for the geometric space of the voids and the water adsorbability of the xanthan gum. Thus, the peak shear strength of the xanthan gum-treated sand becomes higher at the initial state rather than re-submerged states due to the thicker (i.e., high xanthan to water content) xanthan gum hydrogels at the initial condition.

Xanthan gum hydrogels transfer to condensed biofilms through drying (dehydration). The biofilm has a flexible and elastic feature, causing it to have a higher peak shear strength while compacting the sand particles closer together (Chang *et al*. 2016a). Even in the residual state, the cohesion and the friction angle is relatively high since there are some breaks in the xanthan gum biofilm. Furthermore, the cohesion and the friction angle increase as the xanthan gum becomes denser because of the xanthan gum fragments.

A biofilm which absorbs water becomes a hydrogel again. However, the main difference between the initial state and the re-submerged state is whether the absorption water amount is limited or not. The hydrogel in the initial state is made by mixing with a fixed amount of water. By comparison, a hydrogel in a re-submerged state can absorb water to its limit. It results in hydrogel swelling, and the inter-particle interaction is diminished because of the swelling pressure. As a result, sand particles become further apart when it is re-submerged in water. The xanthan gum-treated sand behaves differently in accordance with the xanthan gum density. In lower density

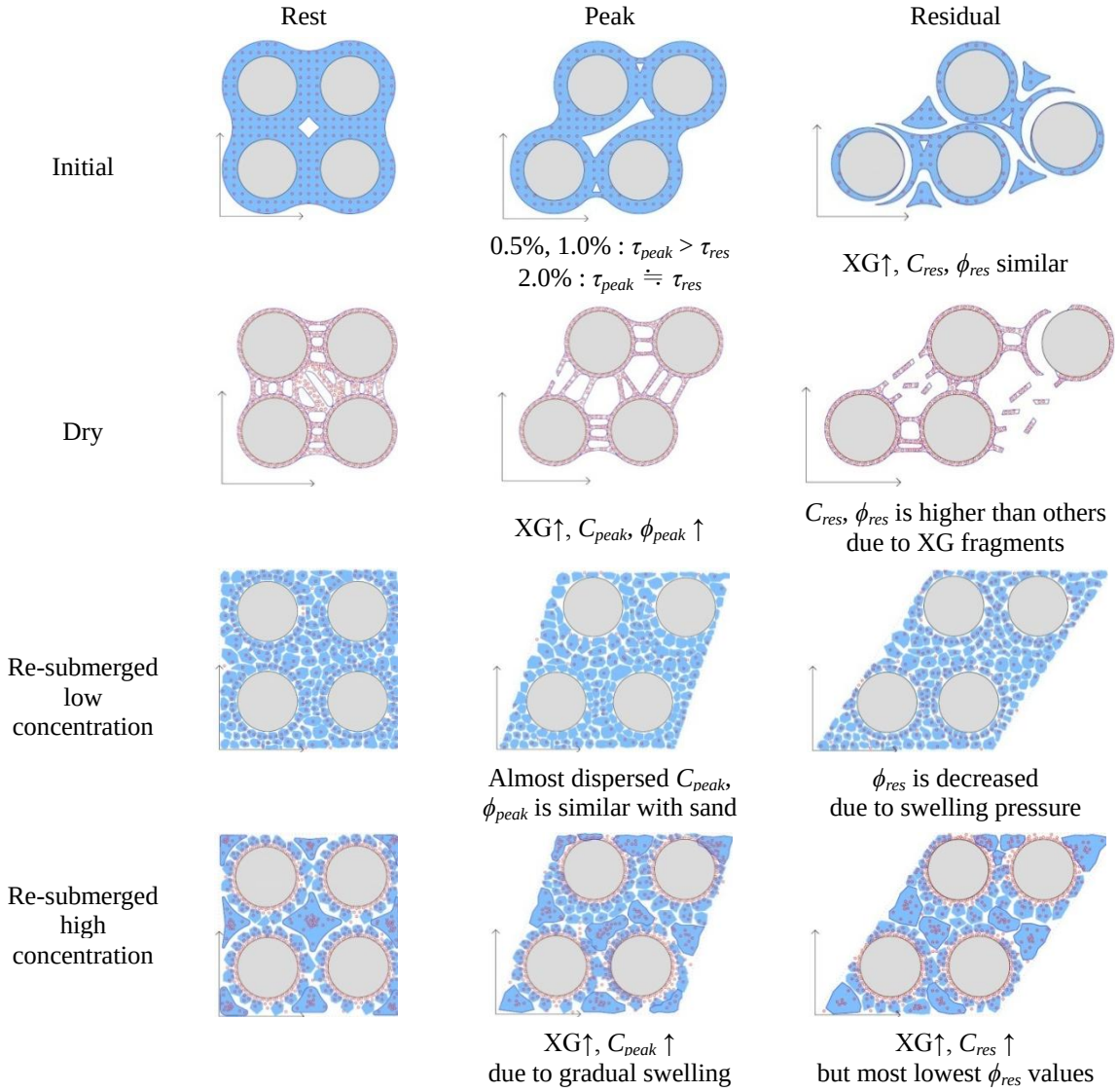

Fig. 8 Schematic diagram of xanthan gum-treated sand (XG = xanthan gum)

conditions, xanthan gum particles, which are attached to the surface of sand particles, are dissolved easily because a biofilm of lower density creates little attraction between the xanthan gum particles. The dissolved xanthan gum particles become crushed, small crumbles, as a form of hydrogel, so that the inter-particle bonding force originating from the hydrogel is relatively small.

In contrast, the inter-particle reaction caused by the hydrogel is more effective in the denser condition because the xanthan gum particles dissolve gradually. The xanthan gum particles, which have had an ionic bonding between particles in the biofilm, dissolve from the rim of the hydrogel. However, the friction force between the hydrogel clusters diminishes as the xanthan gum content increases because the xanthan gum hydrogel behaves like lubricants whose characteristic originates from its pseudo-plasticity.

5. Conclusions

The effects of xanthan gum as an environmentally friendly soil improvement material are verified in this research, specifically in regards to the behavior according to the xanthan gum hydrogel phase—initial, dry, and re-submerged conditions.

First of all, the dried xanthan gum-treated sand has a remarkably high peak shear strength (τ_{peak}); concurrently, its δ-ε_v relationship presents lower dilatancy as the xanthan gum content is increased. It imposes that the dried xanthan gum-treated sand behavior is affected by its rigidity, that is, continuity of cementation materials. This can be explained by the biofilm which is formed when the xanthan gum biopolymer is dehydrated and has a flexible characteristic, so that the ductile behavior occurs. The inter-granular matrix of the xanthan gum-treated sand is effective when more than 1.0% xanthan gum is treated. The comparative gypsum-treated sand shows brittle behavior; therefore, it proves that its strain is not effective for shearing. Moreover, the peak strength (τ_{peak}) of the 10% gypsum-treated sand is lower than the xanthan-treated sand regardless of the xanthan gum content. It means that the gypsum treatment of 10% is not sufficient to improve soil strength adequately. Furthermore, the crushed xanthan gum fragment has a role of ductility in contrast to that of the gypsum which crumbles, and which is proven by brittle behavior, so that the peak strength of the xanthan gum-treated sand is larger than that of the gypsum-treated sand.

The xanthan gum-treated sand behaves differently according to the xanthan gum hydrogel phase variation. In the initial condition, the xanthan gum hydrogel forms a uniformly dissolved matrix by hydrogen bonding. When the xanthan gum is thinner in the hydrogel, the inter-particle reaction is dominant in contrast to that of the shearing band which is formed by the hydrogel. In contrast, the shearing band force is superior in the case of the xanthan gum being dense. As a result, the xanthan gum loosely dissolved sand—2.5% and 5.0%—shows peak behavior although residual behavior in the highly dense xanthan gum-treated sand—10.0%. As the xanthan gum hydrogel is highly concentrated, the peak cohesion increases, though the peak friction angle shows little difference. It reveals that the xanthan gum-treated sand in the initial state, which is tested immediately after mixing, is influenced not by its interlocking but by its viscosity, especially when the xanthan gum concentration is larger than 2.5%. Furthermore, the xanthan gum hydrogel forms a continuous matrix by hydrogen bonding. When the shearing force is applied, the gel is crushed into crumbs and ionic bonding is caused by van der Waals interaction between the hydrogel crumbs. Therefore, the cohesion is increased although the friction angle is unchanged, as the xanthan gum is denser.

When the dried xanthan gum-treated sand is re-submerged, the biopolymer treated sand shows a unique behavior. Only in the case of 2.0% xanthan gum treatment is peak shear strength (τ_{peak}) of the re-submerged condition higher than that of the initial condition. This can be explained by gradual and incomplete swelling. It means that the biofilm has a strong ionic bonding; it is partially dissolved when the biofilm is re-submerged into water and some of the xanthan gum elements become detached when the treated xanthan gum is dense. Therefore, the viscous behavior occurs in high density condition. In contrast, the friction angle decreases as the xanthan gum content increases in both the peak state and the residual state because the swollen xanthan gum hydrogel plays a role as a lubricant, i.e., pseudo-plasticity. Moreover, cohesion does not see a difference between the peak state and the residual state because of structural disturbance which originates from the non-uniform hydrogel structure. Meanwhile, the xanthan gum is dissolved in an unlimited amount of water, so that the peak shear strength is lower than that of the initial condition which contains a specific amount of water.

Consequently, the xanthan gum has an improving effect when the content is more than 1.0% regardless of the hydrogel phase. The biofilm which is formed by drying the xanthan gum-treated sand shows remarkable improvement because of its flexible characteristic—its fragments as ductile elements. The xanthan gum-treated sand in the initial state proves that the shearing behavior is determined according to which mechanism is dominant—the interlocking effect or the shearing band caused by the hydrogen bonding of the hydrogel. The xanthan gum-treated sand behaves uniquely in the case of the re-submerged condition. Because of the gradual swelling, viscous behavior is presented in the case of high xanthan gum concentration. Meanwhile, the friction angle decreases as the xanthan gum content increases because the xanthan gum has a pseudo-plastic characteristic.

Acknowledgments

The research described in this paper was financially supported by a National Research Foundation of Korea (NRF) grant funded by the Korean government (MSIP) (No. 2015R1A2A2A03006268), by a grant (16AWMP-B114117-01-000000) from the Water Management Research Program funded by the Ministry of Land, Infrastructure, and Transport of the Korean government.

References

Ahn, T.B. (2010), "Effects of DCM column properties in softground on stabilities of underground roadway", *KSCE J. Civil Eng.*, **30**(2C), 77-84.

ASTM D3080 / D3080M-11 (2011), Standard test method for direct shear test of soils under consolidated drained conditions; ASTM International, West Conshohocken, PA, USA.

Ayeldeen, M.K., Negm, A.M. and El Sawwaf, M.A. (2016), "Evaluating the physical characteristics of biopolymer/soil mixtures", *Arab. J. Geosci.*, **9**(5), 1-13.

Bell, F.G. (1996), "Lime stabilization of clay minerals and soils", *Eng. Geol.*, **42**(4), 223-237.

Bergado, D.T. (1996), *Soft Ground Improvement: In Lowland and Other Environments*, ASCE Press, New York, NY, USA.

Boardman, D., Glendinning, S. and Rogers, C. (2001), "Development of stabilisation and solidification in lime–clay mixes", *Geotechnique*, **51**(6), 533-543.

Broms, B. and Boman, P, (1975), "Lime stabilized columns", *Proceedings of the 5th Asian Regional Conference on Soil Mechanics and Foundation Engineering*, Bangalore, India, December, pp. 227-234.

Casas, J.A., Santos, V.E. and García-Ochoa, F. (2000), "Xanthan gum production under several operational conditions: molecular structure and rheological properties☆", *Enzyme Microb. Tech.*, **26**(2-4), 282-291.

Chang, I. and Cho, G.-C. (2012), "Strengthening of Korean residual soil with β-1,3/1,6-glucan biopolymer", *Constr. Build. Mater.*, **30**, 30-35.

Chang, I. and Cho, G.-C. (2014), "Geotechnical behavior of a β-1,3/1,6-glucan biopolymer-treated residual soil", *Geomech. Eng., Int. J.*, **7**(6), 633-647.

Chang, I., Im, J. and Cho, G.-C. (2016a), "Geotechnical engineering behaviors of gellan gum biopolymer treated sand", *Can. Geotech. J.*, **53**(10), 1658-1670.

Chang, I., Im, J. and Cho, G.-C. (2016b), "Introduction of microbial biopolymers in soil treatment for future environmentally-friendly and sustainable geotechnical engineering", *Sustainability*, **8**(3), 251.

Chang, I., Im, J., Prasidhi, A.K. and Cho, G.-C. (2015a), "Effects of Xanthan gum biopolymer on soil strengthening", *Constr. Build. Mater.*, **74**, 65-72.

Chang, I., Jeon, M. and Cho, G.-C. (2015b), "Application of microbial biopolymers as an alternative

construction binder for earth buildings in underdeveloped countries", *Int. J. Polym. Sci.*, **9**.
Chang, I., Prasidhi, A.K., Im, J. and Cho, G.-C. (2015c), "Soil strengthening using thermo-gelation biopolymers", *Constr. Build. Mater.*, **77**, 430-438.
Chang, I., Prasidhi, A.K., Im, J., Shin, H.-D. and Cho, G.-C. (2015d), "Soil treatment using microbial biopolymers for anti-desertification purposes", *Geoderma*, **253-254**, 39-47.
Choate, W.T. (2003), "Energy and emission reduction opportunities for the cement industry", *Energy Emission Reduction Opportunities for the Cement Industry*, BCS, Incorporated.
Cole, D., Ringelberg, D. and Reynolds, C. (2012), "Small-Scale Mechanical Properties of Biopolymers", *J. Geotech. Geoenviron. Eng.*, **138**(9), 1063-1074.
Comba, S. and Sethi, R. (2009), "Stabilization of highly concentrated suspensions of iron nanoparticles using shear-thinning gels of xanthan gum", *Water Res.*, **43**(15), 3717-3726.
Das, B.M. and Sobhan, K. (2014), *Principles of Geotechnical Engineering*, Cengage Learning, Australia.
Druss, D.L. (2005), *Challenge of Employing Deep Mixing Methods ill the US*; Deep Mixing.
García, M.C., Alfaro, M.C., Calero, N. and Muñoz, J. (2011), "Influence of gellan gum concentration on the dynamic viscoelasticity and transient flow of fluid gels", *Biochem. Eng. J.*, **55**(2), 73-81.
Ham, S., Kwon, T., Chang, I. and Chung, M. (2016), "Ultrasonic P-Wave Reflection Monitoring of Soil Erosion for Erosion Function Apparatus", *Geotech. Test. J.*, **39**(2), 301-314.
Havlica, J. and Sahu, S. (1992), "Mechanism of ettringite and monosulphate formation", *Cement Concrete Res.*, **22**(4), 671-677.
Horpibulsk, S., Rachan, R., Suddeepong, A. and Chinkulkijniwat, A. (2011), "Strength development in cement admixed Bangkok clay: Laboratory and field investigations", *Soils Found.*, **51**(2), 239-251.
Lin, K.Q. and Wong, I.H. (1999), "Use of deep cement mixing to reduce settlements at bridge approaches", *J. Geotech. Geoenviron. Eng.*, **125**(4), 309-320.
Larsson, S., Rothhämel, M. and Jacks, G. (2009), "A laboratory study on strength loss in kaolin surrounding lime–cement columns", *Appl. Clay Sci.*, **44**(1-2), 116-126.
Malekpoor, M. and Poorebrahim, G. (2014), "Comparative study on the behavior of lime-soil columns and other types of stone columns", *Geomech. Eng., Int. J.*, **7**(2), 133-148.
Mitchell, J.K. and Soga, K.B. (2005), *Fundamentals of Soil Behavior*, Wiley, Hoboken, NJ, USA.
Nugent, R.A., Zhang, G.P. and Gambrell, R.P. (2009), "Effect of exopolymers on the liquid limit of clays and its engineering implications", *Transport. Res. Record*, **2101**, 34-43.
Plank, J. (2005), "Applications of biopolymers in construction engineering", *Biopolymers Online*, Wiley-VCH Verlag GmbH & Co. KGaA.
Sherwood, P.T. (1993), *Soil Stabilization with Cement and Lime*, HMSO, London, UK.
Shooshpasha, I. and Shirvani, R.A. (2015), "Effect of cement stabilization on geotechnical properties of sandy soils", *Geomech. Eng., Int. J.*, **8**(1), 17-31.
U.S. Energy Information Administration (2015), International Energy Statistics; (U.S. Department of Energy, Ed.), Washington, DC, USA.